



PII S0016-7037(00)01030-X

Iron local structure in tektites and impact glasses by extended X-ray absorption fine structure and high-resolution X-ray absorption near-edge structure spectroscopy

GABRIELE GIULI,^{1,2} GIOVANNI PRATESI,^{3,4,*} CURZIO CIPRIANI,³ and ELEONORA PARIS^{1,2}¹Dipartimento di Scienze della Terra, Università di Camerino, Via G. III da Varano, 62032 Camerino (MC), Italy²Unità Istituto Nazionale Fisica della Materia (INFM), Università di Camerino, Camerino, Italy³Museo di Storia Naturale, sezione di Mineralogia e Litologia, Università di Firenze, Via G. la Pira 4, 50121 Firenze, Italy⁴Museo di Scienze Planetarie della Provincia di Prato, Prato, Italy

(Received April 10, 2002; accepted in revised form June 24, 2002)

Abstract—The local structure of iron in three tektites has been studied by means of Fe K-edge extended X-ray absorption fine structure (EXAFS) and high-resolution X-ray absorption near-edge structure (XANES) spectroscopy in order to provide quantitative data on $\langle\text{Fe-O}\rangle$ distance and Fe coordination number. The samples studied are a moldavite and two australasian tektites. Fe model compounds with known Fe oxidation state and coordination number were used as standards in order to extract structural information from the XANES pre-edge peak. EXAFS-derived grand mean $\langle\text{Fe-O}\rangle$ distances and Fe coordination numbers for the three tektite samples are constant within the estimated error ($\langle\text{Fe-O}\rangle = 2.00 \text{ \AA} \pm 0.02 \text{ \AA}$, CN = 4.0 ± 0.4). In contrast to other data from the literature on Fe-bearing silicate glasses, the tektites spectra could not be fitted with a single Fe-O distance, but rather were fit with two independent distances ($2 \times 1.92 \text{ \AA}$ and $2 \times 2.08 \text{ \AA}$). High-resolution XANES spectra of the three tektites display a pre-edge peak whose intensity is intermediate between those of staurolite and grandidierite, thus suggesting a mean coordination number intermediate between 4 and 5. Combining the EXAFS and XANES data for Fe, we infer the mean coordination number to be close to 4.5.

Comparison of the tektites XANES spectra with those of a suite of different impact glasses clearly shows that tektites display a relatively narrow range of Fe oxidation state and coordination numbers, whereas impact glasses data span a much wider range of Fe oxidation states (from divalent to trivalent) and coordination numbers (from tetra-coordinated to esa-coordinated). These data suggest that the tektite production process is very similar for all the known strewn fields, whereas impact glasses can experience a wide variety of different temperature–pressure–oxygen fugacity conditions, leading to different Fe local structure in the resulting glasses. These data could be of aid in discriminating between tektite-like impact glasses and impact glasses *sensu strictu*. Copyright © 2002 Elsevier Science Ltd

1. INTRODUCTION

Tektites are natural silicate glasses usually having rounded shapes (e.g., spheres, teardrops, dumbbells, disks) that can be found scattered over wide areas called strewn fields. Although most of them superficially resemble obsidians, tektites can be distinguished from the latter by their chemistry and petrography (Glass, 1990). Despite the controversy on their origin (see O’Keefe, 1976, and references therein), most investigators now believe tektites to be formed during hypervelocity impact of extraterrestrial objects onto the Earth’s surface (see Montanari and Koeberl, 2000, and references therein).

Glass structure (i.e., cation coordination number) is affected by the pressure (P)–temperature (T) conditions existing during the glass formation process (Stebbins and McMillan, 1989; Paris et al., 1994; Mysen and Neuvill, 1995; Yarger et al., 1995). In particular, pressure tends to increase the mean coordination number of the cations present. Al coordination in glasses is a particularly interesting case because of the vast literature on the dependence of Al coordination vs. glass composition and the P and T of synthesis. In particular, for what concerns the compositions usually found in terrestrial silicate glasses, Al is usually tetra-coordinated by oxygen in silicate

glasses formed at room pressures, whereas more and more high-coordinated species (fivefold and sixfold coordinated Al) tend to form as the pressure increases. By comparing Al coordination data of impact glasses with those of synthetic systems, it is thus possible to understand whether the melt/glass transition occurred in a low-pressure regime (Giuli et al., 2000) or if there are portions of the glass that still record their high-pressure origin (Pratesi et al., 2001).

The relation between P-T conditions and Fe’s structural role in synthetic glasses has not been as extensively studied as for Al. In particular, although many studies have focused on the Fe oxidation state, fewer have focused on both Fe oxidation state and coordination number. In this case, the situation is complicated by the fact that Fe can have a variety of possible roles (Fe²⁺ in four-, five-, six-, and eightfold coordination and Fe³⁺ in four-, five-, and sixfold coordination). In view of the great variety of Fe structural roles in silicate glasses, it is interesting to investigate Fe coordination numbers along with Fe oxidation states to provide a further parameter that, although not yet directly linked to the glass formation conditions, is still related to the P, T, and f_{O_2} condition.

Because iron is a useful probe to obtain information on the formation conditions of tektites, there have been several studies on Fe oxidation states and coordination numbers (Korotayeva et al., 1985; Fudali et al., 1987; Aramu et al., 1994; Thorpe et al., 1994; Dunlap, 1997; Dunlap et al., 1998; Rossano et al.,

* Author to whom correspondence should be addressed (gabriele.giuli@unicam.it).

Table 1. Tektites, impactites, and model compounds studied.

Sample	Provenance	Fe oxidation state, coordination number
Moldavite ^a	Chlum (Czech Republic)	
Australite ^b	Australia	
Cambodianite ^c	Cambodia	
Libyan Desert Glass ^d	Great Sand Sea (Egypt)	
Suevite ^e	Ries crater (Germany)	
Wabar ^f	Wabar crater (Saudi Arabia)	
Aouelloul ^g	Aouelloul crater (Mauritania)	
Darwin Glass ^h	Mt. Darwin crater - Tasmania	
Irghizite ⁱ	Zhamanshin crater - Kazakhstan	
Staurolite	Canton Ticino (CH)	Fe ²⁺ [4]
FeMg-akermanite	Synthetic	Fe ²⁺ [4]
Grandidierite	Madagascar	Fe ²⁺ [5]
Kirschsteinite	Synthetic	Fe ²⁺ [6]
Andradite	Val Malenco (I)	Fe ³⁺ [6]

Catalog number (samples from the collections of Museo di Storia Naturale, Sez. Mineralogia e Litologia Università di Firenze): ^a 2669RI, ^b 2663RI, ^c 2664RI, ^d 2670RI; (samples from the collections of the Museum of Planetary Sciences, Provincia di Prato): ^e 1601, ^f 1602, ^g 1603, ^h 1604, and ⁱ 1605.

1999). However, there is still no consensus on the Fe coordination state in tektites. Earlier studies interpreted most of the Fe to be divalent and in octahedral coordination (Korotayeva et al., 1985) or with minor amounts in tetrahedral coordination (Dunlap, 1997; Dunlap et al., 1998). More recently, Rossano et al. (1999) analyzed the Mössbauer spectra of three tektites, and, considering the independent distribution of isomer shift and quadrupole splitting parameters, they interpreted the divalent iron to be distributed between fivefold and fourfold coordinated sites, the former prevailing over the latter. Furthermore, because of the similarity between the Mössbauer parameters of the tektites and those of grandidierite (Seifert and Olesch, 1977), they inferred the fivefold sites to be trigonal bipyramids.

In this study we analyzed extended X-ray absorption fine structure (EXAFS) spectra of three tektites to obtain quantitative data on mean Fe-O distance and Fe coordination number. Moreover, high-resolution X-ray absorption near-edge structure (XANES) spectra of the same samples provided additional information on the coordination state of Fe in the tektites

studied. The data on tektites have been compared with those on a group of impact glasses to test whether diverse formation conditions, as presumably there are in craters with different dimension, age, target rock composition, and melt/rock ratio, can produce substantial differences in the iron local structure (oxidation state and coordination number).

This work is part of a larger project that aims to determine the role of Al, Si, Fe, Mn, and possibly S in tektites and impact glasses.

2. SAMPLES AND EXPERIMENTAL

The samples we studied comprised three tektites (Table 1) that came from different localities and belonged to the collection of the Natural History Museum of the University of Florence: a moldavite from the Central European strewn field, and a cambodianite and an australite from the Australasian strewn field. The tektite samples were chosen from those available so as to represent a suite of different compositions spanning a relatively wide range in alkali and alkaline earth content (Table 2). Besides tektites, a suite of impact glasses, including Darwin glass from the Darwin crater (Australia), irghizite from the Zhamanshin crater (Kazakhstan), Wabar glass (Saudi Arabia), suevite glass from the Ries crater, (Germany), Libyan Desert glass (LDG) from the Great Sand Sea (Egypt), and glass from the Aouelloul crater (Mauritania), were also studied in order to evaluate differences and analogies. All the samples were previously examined by optical microscopy and by scanning electron microscopy to verify the absence of crystals and to select a homogeneous portion for X-ray Absorption Spectroscopy (XAS) measurement.¹ Chemical compositions were obtained by means of a JEOL JXA 8600 electron microprobe operating at 15.0 kV and 10.0 nA and with the electron beam defocused to a radius of 20 μm . The standards used were as follows: albite for Si and Na, anorthite for Al, ilmenite for Fe and Ti, chromite for Cr, bustamite for Mn, diopside for Ca, olivine for Mg, and sanidine for K. Data were corrected according to the Bence and Albee (1968) algorithm. Tabulated data are averages of seven individual analyses.

The standards used for XAS measurements are a staurolite

¹ The suevite sample was found to contain plagioclase and quartz crystals.

Table 2. Major element chemical composition^a (oxide wt%) of the tektites and impact glasses studied.

Element	Moldavite	Australite	Cambodianite	Libyan desert glass	Suevite	Wabar	Aouelloul	Darwin Glass	Irghizite
SiO ₂	76.62 (46)	71.06 (43)	72.63 (44)	98.44 (29)	65.34 (26)	81.97 (25)	86.69 (26)	85.19 (26)	75.29 (23)
Al ₂ O ₃	10.56 (20)	14.09 (25)	13.53 (24)	0.55 (0)	15.72 (8)	2.59 (5)	6.54 (5)	7.83 (5)	10.08 (10)
Cr ₂ O ₃	0.00 (0)	0.01 (0)	0.02 (0)	0.00 (0)	0.02 (0)	0.03 (0)	0.02 (0)	0.02 (0)	0.05 (1)
FeO	1.98 (12)	4.80 (30)	4.56 (30)	0.09 (3)	4.77 (10)	12.11 (23)	2.27 (6)	2.17 (6)	5.44 (15)
MnO	0.06 (2)	0.07 (2)	0.09 (2)	0.00 (0)	0.12 (3)	0.00 (0)	0.04 (1)	0.02 (0)	0.09 (2)
CaO	3.39 (16)	3.15 (15)	1.67 (8)	0.00 (0)	3.54 (4)	0.93 (4)	0.37 (2)	0.08 (1)	2.45 (5)
MgO	2.31 (12)	2.36 (12)	1.88 (10)	0.00 (0)	2.50 (4)	0.33 (3)	1.23 (3)	1.34 (2)	2.60 (5)
K ₂ O	3.31 (16)	2.24 (12)	2.54 (12)	0.01 (0)	4.03 (7)	0.90 (3)	2.01 (5)	1.59 (4)	2.01 (5)
Na ₂ O	0.40 (6)	1.20 (8)	1.39 (8)	0.01 (0)	3.06 (11)	0.37 (5)	0.31 (5)	0.36 (9)	1.05 (6)
TiO ₂	0.35 (4)	0.81 (4)	0.75 (4)	0.08 (2)	0.75 (3)	0.09 (2)	0.46 (2)	0.62 (3)	0.75 (4)
Total	98.98	99.79	99.06	99.18	99.85	99.32	99.94	99.22	99.81

^a As measured by electron microprobe; uncertainties in the last decimal place are shown in parentheses.

from Canton Ticino (CH) and a synthetic Fe-akermanite for Fe^{2+} in tetrahedral coordination, a grandidierite from Madagascar for Fe^{2+} in trigonal dipyramidal coordination, a synthetic kirschsteinite, and a siderite from Erzberg (A) for Fe^{2+} in octahedral coordination and a natural andradite for Fe^{3+} in octahedral coordination. The natural standards were separated by hand from thumb-sized crystals; we chose the clearest portions to avoid impurities. All the standards were checked for purity by both optical microscopy and X-ray diffraction.

Samples for absorption measurement were prepared by smearing finely ground powder on a kapton tape. EXAFS spectra were collected at the beamline SB04-1 of the SPEAR storage ring (Stanford Synchrotron Radiation Laboratory, Stanford, California, USA) operating at 3 GeV with ring current ranging from 65 to 90 mA. Radiation was monochromatized by means of two flat Si (111) crystals. Spectra were recorded in step-scan mode measuring the incident beam intensity with a ionization chamber and the fluorescence yield with a Lytle detector. Scans ranged from 7000 to 7700 eV with energy steps ranging from 0.5 to 2.0 eV (in the edge region and EXAFS region, respectively) and 3-s counting time. High-resolution XANES spectra were collected at the beamline BM-8 of the European Synchrotron Radiation Facility storage ring (Grenoble, France) operating at 6 GeV and with ring current ranging from 50 to 100 mA. Radiation was monochromatized by means of two channel-cut Si (311) crystals. Spectra were recorded in step-scan mode measuring the incident beam intensity with a ionization chamber and the fluorescence yield with a high purity Ge detector. Scans ranged from 7000 to 7300 eV with 0.2-eV step and 8-s counting time.

3. DATA REDUCTION

EXAFS data reduction and analysis were performed by means of the GNXAS software package (Filipponi and Di Cicco, 2000). This program extracts the EXAFS signal ($\chi(k)$) from the raw spectrum without performing Fourier filtering and thus avoids possible biases deriving from incorrect background subtraction. The theoretical amplitudes and phase shifts are calculated ab initio according to the muffin-tin approximation. The Hedin-Lundquist complex potential (Hedin and Lundquist, 1971) was used for the exchange-correlation potential of the excited state. The amplitude reduction factor (S_0^2) has been fixed to 0.83, in agreement with the values observed for several crystalline standard (G. Giuli, unpublished data). This value is in agreement to that used by Farges et al. (1994) of 0.82, and that used by Di Cicco et al. (1994) of 0.85.

Experimental XANES spectra were reduced by background subtraction with a linear function and then normalized for atomic absorption on the average absorption coefficient of the spectral region from 7150 to 7300 eV. Energy was calibrated against a standard of Fe metal (7112 eV). The threshold energy was taken as the first maximum of the first derivative of the spectra, whereas peak positions were obtained by calculating the second derivative of the spectra. Pre-edge peak analysis was carried out following the same procedure reported in Wilke et al. (2001). The pre-edge peak was fitted by a sum of pseudo-Voigt function, and the integrated intensities along with centroid energies were compared with those of the standards analyzed here and others from the literature (Wilke et al., 2001;

Farges, 2001) to extract information on Fe oxidation state and coordination number in the glasses studied.

4. RESULTS

4.1. Composition

The chemical composition of the samples examined is reported in Table 2 in the form of weight percent oxide content. On the whole, the compositions reported in this study are in agreement with those found in the literature for analogous samples. In particular, the composition of the moldavite sample is similar to that of sample CLM 1 of Meisel et al. (1997), whereas those of the australite and cambodianite fall within the ranges reported by Koeberl (1990) for tektites of similar provenance. Also, the impact glass compositions agree with those previously reported in the literature (for details, see Koeberl, 1997, and Barrat et al., 1997, for the LDG; Mittlefehldt et al., 1992, for the Wabar glass; Koeberl and Auer, 1991, for the Aouelloul glass; Meisel et al., 1990, for the Darwin glass; and Bouska et al., 1981, for the irghizite). As for the totals, although they were somewhat lower than expected for anhydrous samples, as impact glasses are, they fall within the ranges already found in the literature.

4.2. EXAFS

Preliminary trials to fit the EXAFS spectra have been performed assuming regular geometries around the absorber in sixfold (octahedron), fivefold (trigonal dipyramid), or fourfold (tetrahedron) coordination. Because those were unsuccessful, further trials involved the refinement of two different distances along with their multiplicity. In particular, the multiplicities of the two distances were allowed to vary independently from 2 to 3; that way, the refined mean coordination number was free to vary from 4 to 6, and thus it was possible to simulate both mixing of two different polyhedra, or distortion of a single polyhedron around the absorber. A successful fit was obtained only when considering two short Fe-O distances and two long ones. A new cluster was then built to calculate the theoretical signals, which consisted of a distorted FeO_4 tetrahedron linked by the corners to four additional SiO_4 tetrahedra in the second coordination shell. The final fit included four Fe-O and two Fe-Si distances (Table 3). The experimental and theoretical $\chi(k)$ signals are shown in Figure 1, whereas the Fourier transforms are shown in Figure 2. The fit is very good, and the absence of residual contributions in the Fourier transform spectra testifies that there are no other structural contributions to be taken into account. In fact, no significant contributions are observed beyond the first coordination shell, except for a small peak due to the Fe-Si distance. The $\langle\text{Fe-O}\rangle$ distances are $2.00 \pm 0.02 \text{ \AA}$, and there are no significant differences between the three tektites. The refined $\langle\text{Fe-O}\rangle$ distance, as well as the individual Fe-O distances (e.g., for australite $2 \times 1.93 \text{ \AA}$ and $2 \times 2.09 \text{ \AA}$), is reasonably close to those of fourfold coordinated Fe^{2+} in staurolite ($2 \times 1.972 \text{ \AA}$, $1 \times 2.041 \text{ \AA}$, $1 \times 2.038 \text{ \AA}$ according to Stahl and Legres, 1990) and is thus consistent with the refined coordination number. To confirm the validity of the refined coordination number, the spectrum of grandidierite was analyzed as well, resulting in a refined coordination number equal to 5.0 ± 0.4 ; the goodness of this result guaran-

Table 3. Essential parameters of the EXAFS refinement.

Element	Moldavite	Cambodianite	Australite
Fe-O (\AA)	1.91 (2)	1.93 (2)	1.93 (2)
σ^2 (\AA^2) ^a	0.0034	0.0022	0.0021
Fe-O (\AA)	2.06 (2)	2.10 (2)	2.09 (2)
σ^2 (\AA^2)	0.0090	0.0098	0.0091
<Fe-O> (\AA)	1.99	2.02	2.01
C.N.	3.96 (40)	4.10 (40)	3.96 (40)
Fe-Si (\AA)	2.73	2.77	2.78
σ^2 (\AA^2)	0.0076	0.0070	0.0148
E_0 (eV) ^b	7119.3	7119.3	7119.3
E_0 (eV) ^c	7117.9	7118.6	7119.7
K range (\AA^{-1})	3.5–12.5	3.5–12.5	3.5–12.5
S_0^2	0.83	0.83	0.83
R^d	0.00000105	0.00000333	0.00000384

^a EXAFS Debye-Waller factor.

^b Experimental value (taken as the maximum in the derivative spectrum).

^c Refined value.

^d Disagreement index (Filipponi and Di Cicco, 2000).

tees that the procedures for data analysis are correct, and that there are no systematic underestimations of the coordination numbers obtained. Further trials involving data analysis in the anharmonic approximation did not improve the quality of the results; furthermore, the refined coefficient for anharmonicity

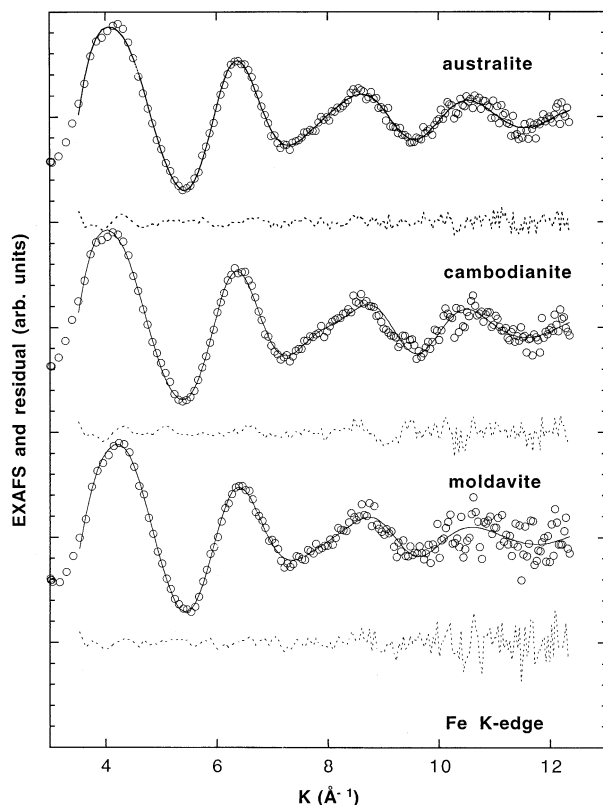


Fig. 1. Comparison between the experimental, theoretical, and residual Fe K-edge EXAFS signals of the tektites studied. The EXAFS signals are weighted by K^2 . Symbols as follows: circles = experimental; solid line = theoretical; dotted line = residual.

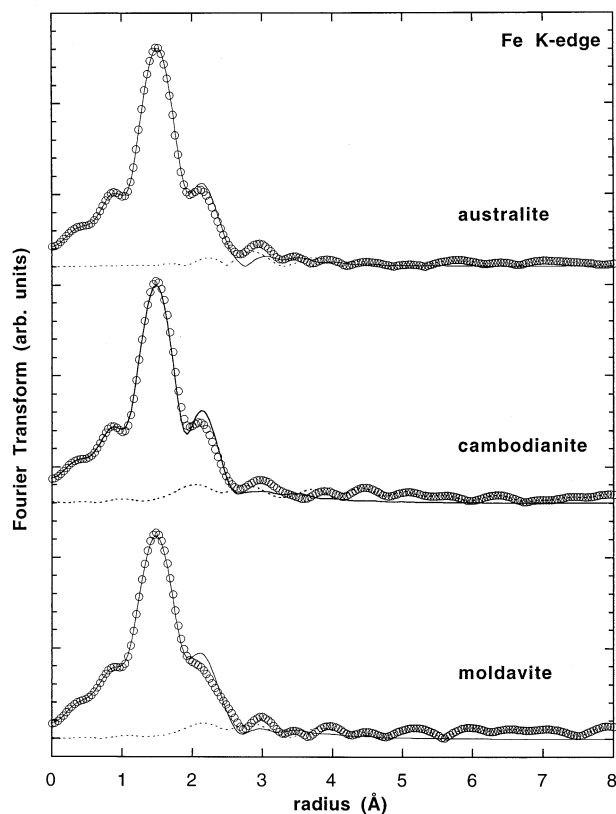


Fig. 2. Comparison between the Fourier transforms of the experimental, theoretical, and residual EXAFS signals of the tektites studied. Symbols as in Figure 1.

was always close to 0.1 and was thus neglected in the final fit. These data are in agreement with other studies performed on synthetic silicate glasses (Cooney and Sharma, 1990; Jackson et al., 1993; Brown et al., 1995; Rossano et al., 2000) where divalent Fe is reported to be mainly tetraordinated.

4.3. XANES

XANES spectra of the Fe model compounds are shown in Figure 3a, and those of the three tektites are shown in Figure 3b. The pre-edge peak (Fig. 4a,b) is the most useful feature to discriminate the oxidation state and coordination number of Fe. This peak represents a $s-d$ like transition and is thus dipole forbidden, but it becomes partially allowed by mixing of the d -states of the transition metal with the p -states of the surrounding oxygen atoms. Its energy position depends mainly on the mean Fe oxidation state, whereas its intensity depends on the geometry around Fe (Calas and Petiau, 1983; Wilke et al., 2000, 2001), so that it will be virtually zero in case of regular octahedral symmetry (O_h) around the absorber, whereas it will reach its maximum in case of tetrahedral coordination (T_d). To extract as much quantitative information as possible from the pre-edge peaks, their integrated intensity is plotted vs. the energy position of their centroids in Figure 5 (Table 4) along

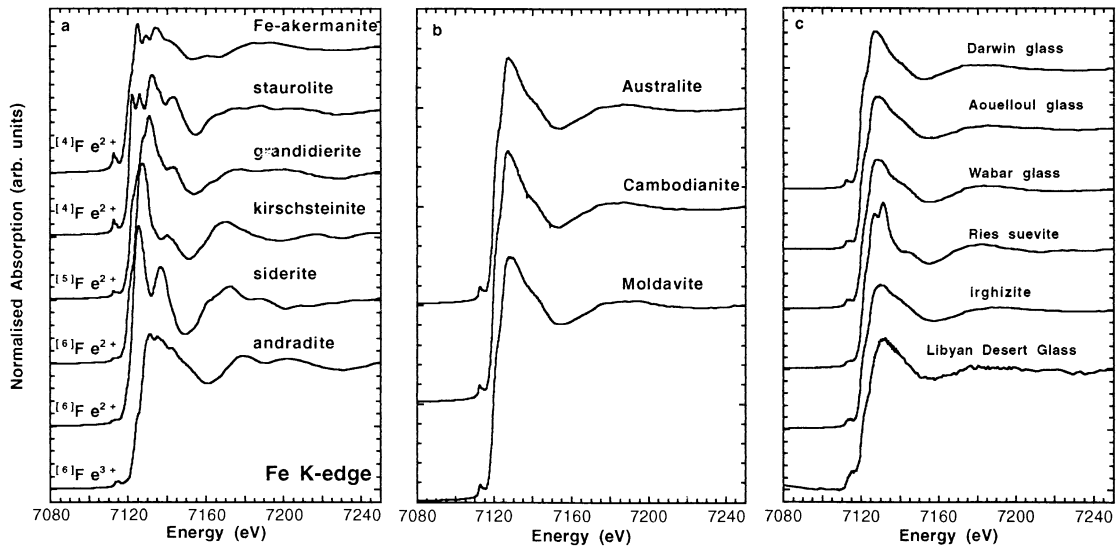


Fig. 3. Experimental Fe K-edge XANES spectra of (a) model compounds with Fe in different oxidation state and coordination numbers; (b) the tektites; and (c) impact glasses studied. The spectra are normalized to one at the high energy side (see text for details).

with those of the standards used in this study and the data reported in Wilke et al. (2001) and Farges (2001).²

In our case, the energy position of the pre-edge peak of tektites is consistent with Fe being mainly divalent. Only the moldavite sample is little shifted to higher energy, possibly the result of some Fe³⁺ contribution. However, given the repro-

ducibility of energy measurement (0.05 to 0.1 eV) and the error in the determination in Fe oxidation state (± 10 mol% according to Wilke et al., 2001) the three tektite samples examined can be said to be indistinguishable from the XAS point of view; the position of the pre-edge peak is thus consistent with Fe oxidation state ranging from 0 to 10 mol% Fe³⁺, in agreement with the data from Fudali et al. (1987). As contributions arising from Fe³⁺ or Fe⁰ were not clearly detected we can exclude their presence in large amounts in our tektite samples (i.e., >10 mol%).

The integrated intensities of the tektite pre-edge peaks are

² As Wilke et al. (2001) and Farges (2001) calibrated the edge energy of Fe metal at 7112.92 eV, their values have been rescaled accordingly in order to be compared with our values. On the whole, there is a good agreement in both energy and integrated intensity in the three sets of standards reported.

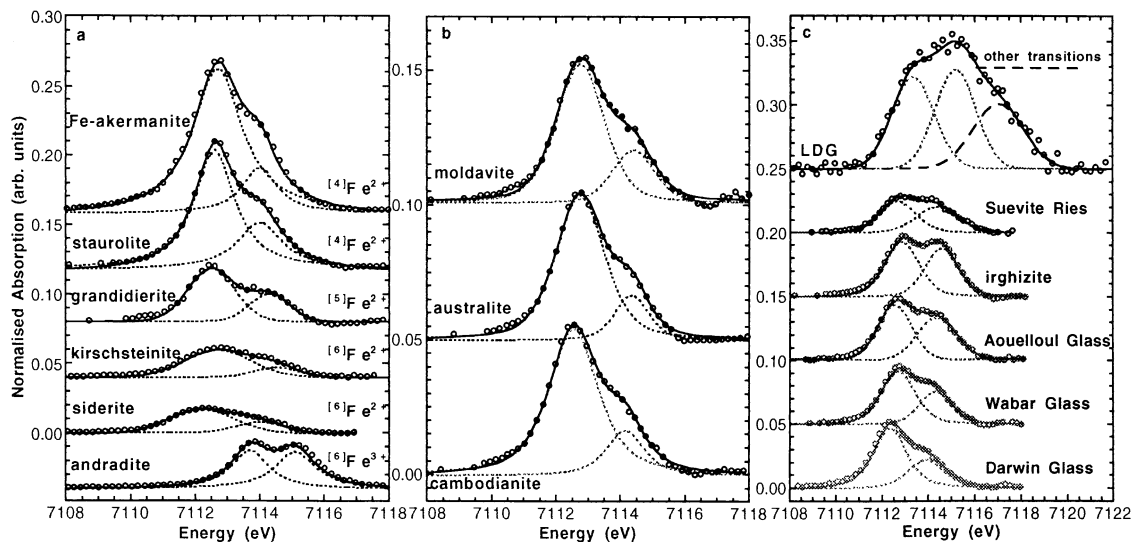


Fig. 4. Pre-edge peak of (a) model compounds with Fe in different oxidation state and coordination numbers, (b) the tektites, and (c) impact glasses studied after background subtraction. The energy scale in (c) has been changed to accommodate the pre-edge peak of the LDG sample.

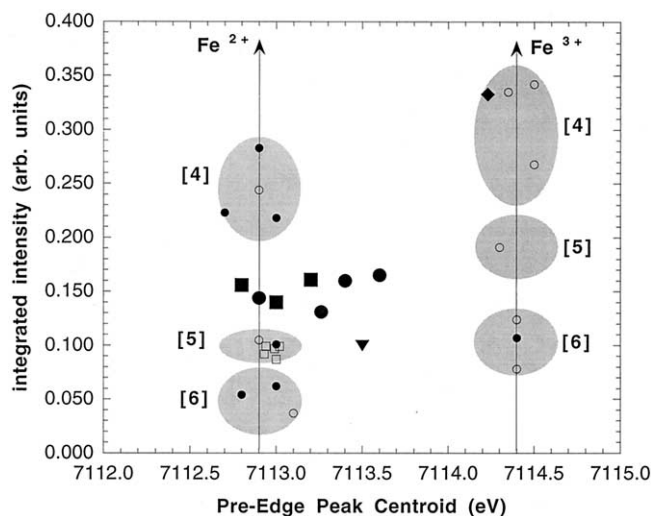


Fig. 5. Plot of the pre-edge peak integrated intensity vs. centroid energy. Solid symbols refer to the samples studied here (squares = tektites; circles = impact glasses; diamond = LDG; triangle = suevite; small circles = model compounds); open symbols refer to the Fe model compounds reported in Wilke et al. (2001) and Farges (2001). The energy of the model compounds reported in the latter references has been rescaled to compensate for the different calibration adopted (see text).

clearly intermediate between those of staurolite and grandierite, thus suggesting a mean coordination number intermediate between 4 and 5. In particular, interpolation of the intensity of the pre-edge peaks of grandierite and staurolite, with the assumption that Fe is present only in fourfold and fivefold coordination (Rossano et al., 1999), would result in mean coordination numbers from ~ 4.5 to 4.8 in the tektites studied. It must be noted that despite the paucity of standards with fourfold and fivefold coordinated iron, there is sometimes a considerable scatter in the pre-edge peak integrated intensity of standards with the same coordination number and oxidation state, especially for tetracoordinated Fe^{2+} and Fe^{3+} . This scatter introduces a large error in the quantitative determination of the coordination number of our samples: although the pre-edge

peaks of standards with $^{57}\text{Fe}^{2+}$ have integrated intensity at or very close to 0.1, the integrated intensity of the pre-edge peaks of standards with $^{57}\text{Fe}^{2+}$ range from 0.218 to 0.283 (Table 4). Thus, depending on which standards are taken into consideration, the resulting coordination number of the tektites examined can lie in the 4.5 to 4.7 range or 4.7 to 4.8 range. Thus, these coordination numbers are to be taken as semiquantitative. Taking into account the error in the EXAFS-derived coordination number ($\sim 4.0 \pm 0.4$) in combination with the results from XANES, we can confidently say the mean Fe coordination number in the tektites examined to be close to 4.5.

XANES spectra of the impact glasses are shown in Figure 3c, and the pre-edge peaks are shown in Figure 4c. The integrated intensities vs. centroid energy of the tektite and impact glasses are plotted together in Figure 5. It can be clearly noted that all the tektites studied group in a very narrow area that lies midway between the standards for Fe^{2+} in [5] coordination and Fe^{2+} in [4] coordination. The same result is found also from EXAFS and high-resolution XANES data of two Ivory Coast tektites (G. Giuli et al., personal communication) and in a number of low-resolution spectra of tektites from the Australasian and North-American Strewn field (unpublished data). In contrast, impact glasses data span over a wide area indicating a variety of Fe oxidation states from (2+ to 3+) and coordination numbers (from [4] to [6]). In particular, although some impact glasses plot in the same region as the tektites (e.g., Darwin glass), the pre-edge peaks of other glasses are clearly displaced to higher energies as a consequence of a noticeable contribution from Fe^{3+} in the sample (e.g., Irghizite and Ries suevite) or even are indicative of Fe to be completely trivalent, as is the case for the LDG sample ($^{57}\text{Fe}^{3+}$).

5. SUMMARY AND CONCLUSIONS

The XAS analysis of three different tektites shows that there are no appreciable differences in the Fe local environment as a function of bulk chemistry and provenance. This conclusion apply also for two Ivory Coast tektites (G. Giuli et al., personal communication) analyzed with the same techniques, and a number of australites and a bediasite analyzed by low-resolution XANES and EXAFS spectroscopy (unpublished data). The EXAFS data allowed us to obtain Fe-O distances for the samples examined. Considering both EXAFS and XANES data, our results clearly suggest that the mean Fe coordination number is close to 4.5, in fair agreement with the Mössbauer data on tektites of Rossano et al. (1999). However, because of the lack of significant multiple scattering contributions in the EXAFS data, we cannot presently assess whether Fe is in a mixture of 4- and 5-coordinated sites or in 4- and 6-coordinated sites.

As concerns impact glasses, the more evident variability, occurring both in iron oxidation state and iron coordination number, is possibly due to different formation environment characterized by a wider range of pressure, temperature, and oxygen fugacity. The wider range of Fe oxidation states and coordination number displayed by impact glasses may be of aid in discriminating between tektite-like impact glasses and impact glasses. It is particularly interesting for what concern the LDG here examined. Previous geochemical studies (Barrat et al., 1997) noted that "it is difficult to define if LDGs are tektites

Table 4. Pre-edge peak features in the samples studied.

Sample	centroid (eV)	Integrated intensity	Fit agreement index (%)
Siderite	7112.8	0.054000	99.84
Kirschsteinite	7113.0	0.062000	99.83
Grandierite	7113.0	0.101000	99.32
Staurolite	7113.0	0.218000	99.88
Fe-Akermanite	7112.9	0.283000	99.84
Andradite	7114.4	0.107000	99.93
Cambodianite	7112.8	0.156000	99.86
Australite	7113.0	0.140000	99.77
Moldavite	7113.2	0.161000	99.71
Ries	7113.5	0.100000	99.75
Darwin-glass	7112.9	0.144000	99.89
Wabar	7113.3	0.131000	99.84
Aouelloul	7113.4	0.160000	99.79
Irghizite	7113.6	0.165000	99.74
LDG	7114.2	0.333000	99.42

or just impact glasses.” In this regard, the LDG sample here examined plots far away from the region of tektite glasses; this suggests that LDG is not a tektite-like impact glass.

These data are important because on one hand, they constitute a basis on which compare other XAS data on impact glasses. On the other hand, where water content and isotopic composition could not be conclusive in determining whether an impact glass is tektite-like or not (Barrat et al., 1997), and glass structure may help to classify impact glasses. Moreover, despite the relatively large error in the determination of the absorber oxidation state (~ 10 mol%), if complemented by similar data at the Mn, V, and S K-edge, they could be useful in further constraining the T- f_{O_2} region where impact glasses formed. It is important to remark that the combined use of EXAFS and high-resolution XANES produces far more accurate structural information than can be obtained with either of these techniques alone.

Acknowledgments—We thank the staff of beamline SB04-1 of SSRL (Stanford, California, USA) and BM-08 (European Synchrotron Radiation Facility, France) for kind assistance during the experiments. We also thank A. Di Cicco for useful criticism and hints on the EXAFS data analysis. We thank A. Mottana, A. Marcelli, and G. Cibin for their help during the EXAFS data collection at SSRL. F. Seifert kindly provided the synthetic Fe-akermanite. Criticism by the three reviewers greatly improved the quality of the manuscript.

Associate editor: C. Koeberl

REFERENCES

- Aramu F., Brovotto P., Maxia V., Salis M., and Spano G. (1994) Mössbauer spectroscopy of tektites. *Nuovo Cimento* **16D**, 623–626.
- Barrat J. A., Jahn B. M., Amossé J., Rocchia R., Keller F., Poupeau G. R., and Diemer E. (1997) Geochemistry and origin of Libyan Desert glasses. *Geochim. Cosmochim. Acta* **61**, 1953–1959.
- Bence A. E. and Albee A. L. (1968) Empirical correction factors for the electron microanalysis of silicates and oxides. *J. Geol.* **76**, 382–402.
- Bouska V., Povondra P., Florenskij P. V., and Randa Z. (1981) Irghizites and zhamanshinites: Zhamanshin Crater, USSR. *Meteoritics* **16**, 171–184.
- Brown G. E., Farges F., and Calas G. (1995) X-ray scattering and X-ray spectroscopy studies of silicate melts. *Rev. Mineral.* **32**, 317–410.
- Calas G. and Petiau J. (1983) Coordination of iron in oxide glasses through high-resolution K-edge spectra: Information from the pre-edge. *Sol. State. Comm.* **48**, 625–629.
- Cooney T. F. and Sharma S. K. (1990) structure of glasses in the systems $Mg_2SiO_4-Fe_2SiO_4$, $Mn_2SiO_4-Fe_2SiO_4$, $Mg_2SiO_4-CaMgSiO_4$, and $Mn_2SiO_4-CaMnSiO_4$. *J. Non Cryst. Solids* **122**, 10–32.
- Di Cicco A., Berrettoni M., Stizza S., Bonetti E., and Cocco G. (1994) Microstructural defects in nanocrystalline iron probed by X-ray absorption spectroscopy. *Phys. Rev. B* **50**, 12386–12397.
- Dunlap R. A. (1997) An investigation of Fe oxidation states and site distributions in a Tibetan tektite. *Hyperf. Interact.* **110**, 217–225.
- Dunlap R. A., Eelman D. A., and Mackay G. R. (1998) A Mössbauer effect investigation of correlated hyperfine parameters in natural glasses (tektites). *J. Non-Cryst. Solids* **223**, 141–146.
- Farges F. (2001) Crystal-chemistry of Fe in natural grandidierites: A XAFS spectroscopy study at the Fe K-edge. *Phys. Chem. Miner.* **28**, 619–629.
- Farges F., Guyot F., Andraut D., and Wang Y. (1994) Local structure around Fe in $Mg_{0.9}Fe_{0.1}SiO_3$ perovskite: An X-ray absorption spectroscopic study at the Fe K-edge. *Eur. J. Miner.* **6**, 303–312.
- Filippini A. and Di Cicco A. (2000) GNXAS: A software package for advanced EXAFS multiple-scattering calculations and data-analysis. *Task Q.* **4**, 575–669.
- Fudali R. F., Dyar M. D., Griscom D. L., and Schreiber D. (1987) The oxidation state of iron in tektite glass. *Geochim Cosmochim Acta* **51**, 2749–2756.
- Giuli G., Pratesi G., Corazza M., and Cipriani C. (2000) Aluminum coordination in tektites: A XANES study. *Am. Mineral.* **85**, 1172–1174.
- Glass B. P. (1990) Tektites and microtektites: Key facts and inferences. *Tectonophysics* **171**, 393–404.
- Hedin L. and Lundquist B. I. (1971) Explicit local exchange-correlation potentials. *J. Phys. C* **4**, 2064.
- Jackson W. E., Waychunas G. A., Brown G. E. Jr., Mustre de Leon J., Conradson S., and Comber J.-M. (1993) High-temperature XAS study of Fe_2SiO_4 : Evidence for reduced coordination of ferrous iron in the liquid. *Science* **262**, 229–233.
- Koeberl C. (1990) The geochemistry of tektites: An overview. *Tectonophysics* **171**, 405–422.
- Koeberl C. (1997) Libyan Desert glass: Geochemical composition and origin. In *Silica '96* (ed. V. de Michele), pp. 115–120. Pyramids. Segrate, Milano I.
- Koeberl C. and Auer P. (1991) Geochemistry of impact glass from the Aouelloul Crater, Mauritania. *Lunar Planet. Sci. Conf.* **22**, 731–732.
- Korotayeva N. N., Polosin A. V., and Malysheva T. V. (1985) The valency and coordination states of iron in tektites and impactites (in Russian). *Geokhimiya* **6**, 899–903.
- Meisel T., Koeberl C., and Ford R. J. (1990) Geochemistry of Darwin impact glass and target rocks. *Geochim. Cosmochim. Acta* **54**, 1463–1474.
- Meisel T., Lange J. M., and Krahenbuhl U. (1997) The chemical variation of moldavite tektites: Simple mixing of terrestrial sediments. *Meteor. Planet. Sci.* **32**, 493–502.
- Mittlefehldt D. W., See T. H., and Horz F. (1992) Dissemination and fractionation of projectile materials in the impact melts from Wabar Crater, Saudi Arabia. *Meteoritics* **27**, 361–370.
- Montanari A. and Koeberl C. (2000) *Impact Stratigraphy. Lecture Notes in Earth Sciences*, Vol. 93. Springer-Verlag.
- Mysen B. and Neuville D. (1995) effects of temperature and TiO₂ content on the structure of $Na_2Si_2O_5-Na_2Ti_2O_5$ melts and glasses. *Geochim. Cosmochim. Acta* **59**, 325–342.
- O’Keefe J. A. (1976) *Tektites and Their Origin*. Elsevier.
- Paris E., Dingwell D., Seifert F., Mottana A., and Romano C. (1994) Pressure-induced coordination change of Ti in silicate glass: A XANES study. *Phys. Chem. Miner.* **21**, 520–525.
- Pratesi G., Capitani D., Cipriani C., Giuli G., and Ziarelli F. (2001) A ²⁹Si-²⁷Al magic-angle spinning NMR study of natural silica glass from the Libyan Desert (Egypt). *J. Non Cryst. Sol.* **279**, 88–92.
- Rossano S., Balan E., Morin G., Bauer J. P., Calas G., and Brouder C. (1999) ⁵⁷Fe Mössbauer spectroscopy of tektites. *Phys. Chem. Minerals* **26**, 530–538.
- Rossano S., Ramos A., Delaye J. M., Creux S., Filippini A., Brouder C., and Calas G. (2000) EXAFS and molecular dynamics combined study of CaO-FeO-2SiO₂ glass: New insight into site significance in silicate glasses. *Europhys. Lett.* **49**, 597–602.
- Seifert F. and Olesch M. (1977) Mössbauer spectroscopy of grandidierite, (Mg,Fe)Al₃BSiO₉. *Am. Mineral.* **62**, 547–553.
- Stahl K. and Legres J. P. (1990) On the crystal structure of staurolite: The X-ray crystal structure of staurolite from the Pyrenees and Brittany. *Acta Cryst* **B46**, 292–301.
- Stebbins J. F. and McMillan P. (1989) Five- and six-coordinated Si in K₂Si₄O₉ glass quenched from 1.9 GPa and 1200°C. *Am. Mineral.* **74**, 965–968.
- Thorpe A. N., Senftle F. E., May L., Barkatt A., Adelhadadi M. A., Marbury G. S., Izett G. A., and Maurrasse F. R. (1994) Comparison of the magnetic properties and Mössbauer analysis of glass from the Cretaceous–Tertiary boundary, Beloc, Haiti, with tektites. *J. Geophys. Res. Planets* **99**, 10881–10886.
- Wilke M., Farges F., Behrens H., Burkhard D., and Petit P. E. (2000) The local environment of Fe in dry and water-bearing silicate glasses. *J. Conf. Abstr.* **5**, 107.
- Wilke M., Farges F., Petit P. E., Brown G. E., and Martin F. (2001) Oxidation state and coordination of Fe in minerals: An Fe K-XANES spectroscopic study. *Am. Mineral.* **86**, 714–730.
- Yarger J. L., Diefenbacher J., Smith K. H., Wolf G. H., Poe B., and McMillan P. F. (1995) Al³⁺ coordination changes in high pressure aluminosilicate liquids. *Science* **270**, 1964–1967.